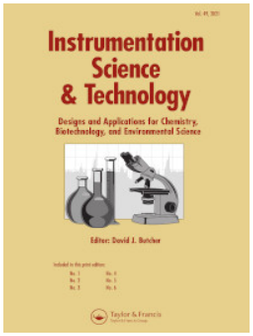

Instrumentation Science & Technology

ISSN: (Print) (Online) Journal homepage: https://www.tandfonline.com/loi/list20

Novel acousto-optical tunable filter (AOTF) based spectropolarimeter for the characterization of auroral emission

Jurgen Vanhamel, Emmanuel Dekemper, Sophie Berkenbosch & Roland Clairquin

To cite this article: Jurgen Vanhamel, Emmanuel Dekemper, Sophie Berkenbosch & Roland Clairquin (2021) Novel acousto-optical tunable filter (AOTF) based spectropolarimeter for the characterization of auroral emission, Instrumentation Science & Technology, 49:3, 245-257, DOI: 10.1080/10739149.2020.1814809

To link to this article: https://doi.org/10.1080/10739149.2020.1814809

Published online: 02 Sep 2020.

INSTRUMENTATION SCIENCE & TECHNOLOGY
2021, VOL. 49, NO. 3, 245–257
https://doi.org/10.1080/10739149.2020.1814809

Taylor & Francis
Taylor & Francis Group

Novel acousto-optical tunable filter (AOTF) based spectropolarimeter for the characterization of auroral emission

Jurgen Vanhamel[a]*, Emmanuel Dekemper[b], Sophie Berkenbosch[a], and Roland Clairquin[a]

[a]Engineering Department, Royal Belgian Institute for Space Aeronomy, Brussels, Belgium; [b]Solar Radiation Department, Royal Belgian Institute for Space Aeronomy, Brussels, Belgium

ABSTRACT

Auroras can be observed at the north and south pole of the Earth. At these locations, the Earth magnetic field enters the atmosphere, causing ionization of the atmospheric constituents. Due to this phenomenon, different optical wavelengths are emitted from these constituents, causing the typical spectacular displays. Several optical wavelengths are representative for the auroral emission. The purpose of the described instrument is to measure the degree of linear polarization of the northern lights, in order to detect and confirm previous observations in which only a low level of polarization was seen. The instrument is capable of resolving the polarization measured at any wavelength in the visible region, using two optical chains, each containing an acousto-optical tunable filter (AOTF). The latter is responsible for the selection of the desired optical wavelength and projects the two polarized beams onto an optical detection system. The driving of the AOTF, using a radio-frequency (RF) signal, is a key-element in establishing trustworthy results. The design of this double RF chain, consisting of a generator, an amplifier, and the necessary circumjacent electronics, is described in the study. In addition, the optical setup of the instrument, together with the detection system is explained. The instrument will be used in the harsh environment of the pole regions, so it must be able to withstand these weather conditions. Hence, a thermal compensation system is necessary and is also described.

KEYWORDS

Acousto-optical tunable filter (AOTF); aurora; radio frequency (RF); spectroscopy

Introduction

Northern lights are a beautiful manifestation of the solar-terrestrial coupling. Produced by the interaction of solar particles with the nitrogen and oxygen atoms in the thermosphere, auroras shine at discrete optical wavelengths corresponding to the electronic transitions which give them birth. The auroral light has a certain level of polarization, which is useful in the

CONTACT Jurgen Vanhamel jurgen.vanhamel@aeronomie.be Engineering Department, Royal Belgian Institute for Space Aeronomy, Ringlaan 3, 1180 Brussels, Belgium.
*ESAT – TELEMIC, Telecommunications and Microwaves, KU Leuven, Leuven, Belgium

frame of predicting space weather[1] or to characterize the atmosphere as a response to particle precipitations.[2]

A level of only a few percent (2–3%) of polarization of one of the major emission lines (the red wavelength is around 630 nm) was measured by Lilensten et al.[3] in 2008. Further measurements of polarized auroral emissions were done by other teams, but need further confirmation due to the observed low signal-to-noise ratio (SNR).[4,5] Consequently, a new concept is pushed forward in order to consolidate these measurements and to further confirm the observations done in the past.

The aurora spectrum consists of many emission lines spanning the ultraviolet (UV), visible, and infrared domain. Among them, the monitoring of the red (630.0 nm) and blue (427.8 nm) lines are the most promising ones for polarization detection, given their strength and their creation mechanism. The 557.7 nm (green line) is expected not to be polarized due to the absence of Zeeman sublevels.[1] Nevertheless, all three spectral lines are taken into account in the instrumental concept. The auroral light polarization should be analyzed in four linear directions, at 0°, 45°, 90°, and 135° in order to determine its Stokes parameters.

To achieve these performance specifications, a double tellurium-dioxide (TeO_2) acousto-optical tunable filter (AOTF) system is designed. The new design consists of a double channel system, each containing an AOTF, an applicable RF driving system, and an optical detection system. This combination leads to an AOTF-based spectropolarimeter for auroras, or ASPA-instrument. A preliminary concept was already presented by Dekemper et al.,[1] but this study describes the designed instrument from an engineering point of view. All necessary engineering concepts are discussed, as well as the testing of the instrument from an electrical, thermal, and optical point of view. Included are some limited results from a field test campaign in February 2020, obtained in Skibotn, Norway.

AOTF principles

The use of an AOTF as an optical wavelength selector is common in several ground- and space-based applications.[6–9] The working principle of an AOTF is based on the interaction between generated sound waves and incoming light inside a birefringent crystal, composed of e.g., TeO_2. If the Bragg matching condition is met,[10] two first-order diffracted light beams appear at the output of the crystal (Figure 1), with orthogonal polarization (the selected spectral intensity is somehow decomposed into orthogonal components). The rest of the light spectrum forms the 0-order. The $+1$ and -1 orders will be of equal intensity only if the incident light is

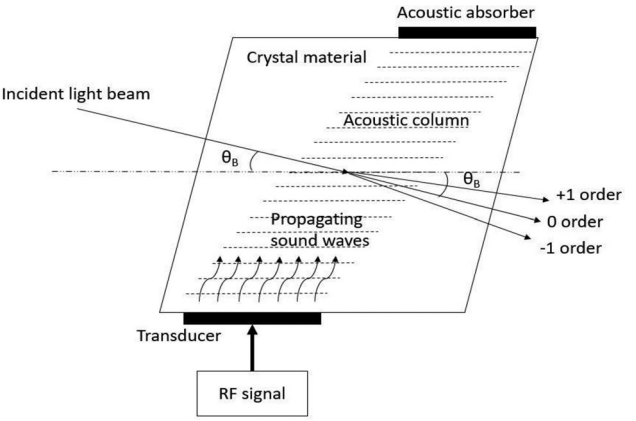

Figure 1. AOTF working principles. Reproduced with permission from reference [17] by OSA Publishing.

Table 1. ASPA-instrument design parameters.

Requirement	Value
Scientific requirements	
Polarized optical wavelength lines	General range 420 – 700 nm [including 557.7 + nm (green), 630.0 nm (red), and 427.8 nm (blue)]
Spectral resolution	1 nm
Field of view	$2^\circ \times 2^\circ$
Temporal resolution	1 min
Observed stokes components	0°, 45°, 90°, and 135°
Engineering requirements	
Frequency range	80 – 105 MHz (green and red) 125 – 155 MHz (blue)
Unwanted spectral components	< −25 dBc
RF output nominal load	50 Ohm
RF generator accuracy	1 kHz
RF resolution	5 kHz
RF generator output power	Maximum +3 dBm
RF power inside AOTF crystal	170 mW (80 – 105 MHz) 60 mW (125 – 155 MHz)
Internal box temperature	Between +10 and +20 °C

unpolarized. The careful analysis of the +1 and −1 beams is the key to determining the degree of linear polarization of specific auroral lines.

In order to generate sound waves inside the crystal, a piezoelectric transducer is mounted on the side of the device, converting the applied RF energy into sound waves. The RF consists of a pure sinewave, variable in frequency, and power level. Hence, a combination of a variable RF generator and RF amplifier is necessary to drive the AOTF at the correct frequency and power.

Instrument requirements

To measure the polarization of the different spectral lines, several practical and scientific requirements need to be met. Based on the scientific requirements, a list of practical design parameters is deduced. In Table 1, the most

prominent scientific and engineering key-elements are listed. A detailed description of these parameters can be found in the following paragraphs.

Scientific requirements

The interesting optical wavelength domains for observing auroral spectral lines are based on Jones[11] and Sigernes et al.[12] Not only are the exact wavelengths of 557.7, 630.0, and 427.7 nm worth measuring, but also the weaker spectral lines in the vicinity. More specific, the instrument should aim at an optical range from 420 to 700 nm. In order to be able to measure in this wide range, all optical elements inside the instrument (AOTF, optical elements, coatings, and detector) should be able to handle this spectral domain. A spectral resolution of 1 nm is chosen in order to resolve the structure of the spectral lines in the most optimal way. In order to focus the instrument onto a small portion of the auroral arc, the field-of-view is limited to 2° by 2°. For the temporal resolution, given the dynamics of auroras, the acquisitions must be performed in less than a minute.

Engineering requirements

The engineering requirements are deduced from the scientific requirements. The RF frequency range is linked to the wavelength of the green, red, and blue lines. The relationship between the diffracted optical wavelength and the RF frequency is given by the approximation:

$$f \cong \frac{\Delta n \ \nu \ \sin 2(\theta_B + \eta)}{\lambda \ \sin \theta_B} \tag{1}$$

in which f is the RF frequency (applied to the transducer of the AOTF), λ the optical wavelength, Δn the absolute difference between the two refractive indices, θ_B the Bragg angle, ν the acoustic wave velocity and α the acoustic wave propagation angle.[13] Additionally, this relationship is shown in Figure 2. The different RF frequency domains, together with the concurrent RF power and corresponding optical wavelength ranges are highlighted as shaded regions (two vertical green regions and two corresponding horizontal orange regions). The selected green and orange areas were the result of a tradeoff, balancing the ranges of the two RF chains with the requested optical lines.

The applied RF signal at the transducer of the AOTF needs to be a pure sinewave in order to select the appropriate optical wavelength. If other RF signals enter the transducer, also other spectral lines will be selected by the AOTF, and the ±1 orders are no longer monochromatic. To avoid this, the unwanted spectral components in the RF output signal need to be suppressed by at least 25 dB compared to the carrier signal.

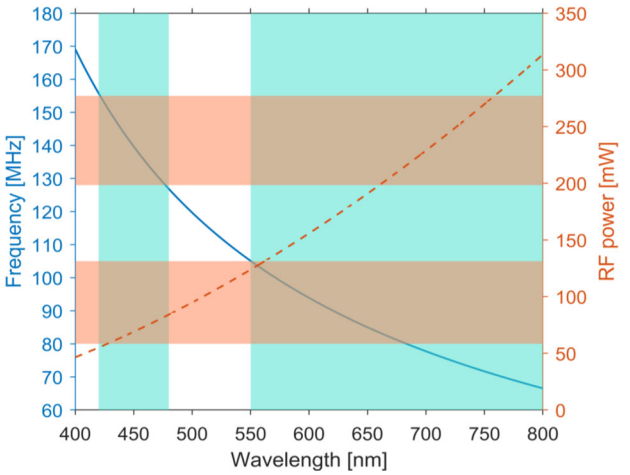

Figure 2. AOTF tuning curve as a function of wavelength (blue solid curve) and acoustic power as a function of the wavelength (red dashed line). The vertical green regions indicate the to-be-observed wavelengths. The horizontal orange regions indicate the corresponding necessary RF frequency (left side Y-axis) and the RF power (right side Y-axis).

The spectral lines have a specific spectral signature.[11,12] Hence, the filter device (AOTF) needs to be able to select the spectral line in an accurate way. Consequently, the applied RF frequency needs to have an accuracy of 1 kHz. The resolution is set at 5 kHz, which is sufficient to precisely reconstruct the spectral signature.

To have a high efficiency inside the AOTF, enabling the detector to capture as many photons as possible, both AOTFs should be driven with a wavelength-depended optimal power level (Figure 2). Due to the used phase-locked-loop (PLL) concept of the RF generator, and a fixed output power level of the RF amplifier, an average power value is chosen for the two dedicated frequency regions highlighted in Figure 2. For building the two optical chains, two commercial AOTFs of Gooch and Housego are used, which are described by Dekemper et al.[8,14] Both AOTFs have a different voltage standing wave ratio (VSWR) behavior. Consequently, power compensation is needed in order to aim at the requested power levels inside the crystal (60 and 170 mW depending on the frequency range). Due to the limited RF amplifier input signal, the RF generator may only apply a maximum output power level of + 3 dBm.

Practical instrument setup

In order to retrieve the four Stokes components at 0°, 45°, 90°, and 135° for polarization detection, a double channel system is used. The double approach is needed due to the limitation of envisaging only two orders using a single AOTF. They represent two of the Stokes components (0°

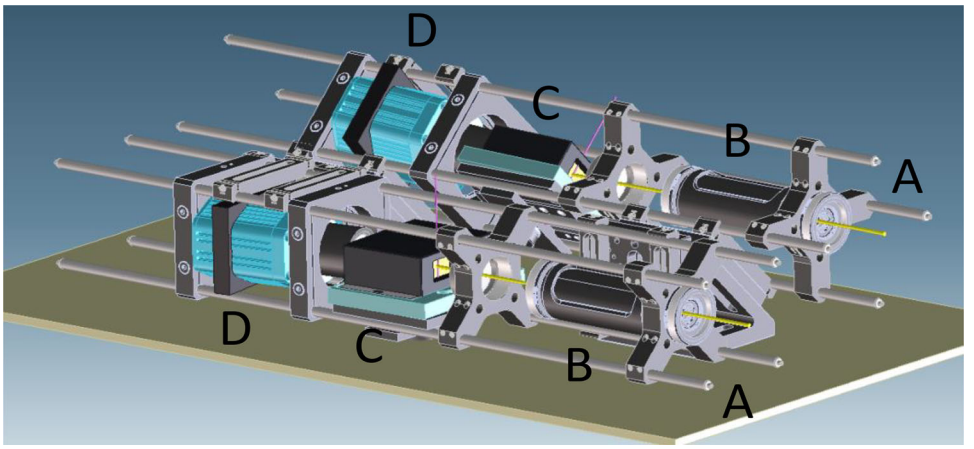

Figure 3. ASPA optical dual-channel concept: (A) entrance pupil, (B) front-end optics, (C) AOTF, and (D) detector.

and 90°). To detect the other two (45° and 135°), an additional identical, but tilted, channel is needed. Each channel consists of a pupil entrance, front-end optics to bundle the light, an AOTF for wavelength selection, and an optical detection system enabling the detection of the +1 and −1 order of the diffracted light beam. Both channels need a relative tilt of 45° in order to retrieve the four polarizations (Figure 3).

Optical setup

Two dedicated optical chains are used. The auroral light enters the instrument *via* the pupils (Figure 3A). Two transparent glass windows are mounted inside the mechanical enclosure of the instrument. After light entering, front-end optics (Figure 3B) focuses the incoming light onto the optical apertures of the AOTFs (Figure 3C). These filters diffract the light into two times a + 1 and −1 order beam. Both double beams are projected onto the cameras (Figure 3D) at the end of the baseplate. Hence, four (two times two) bundles of light are of interest and are projected onto the complementary metal oxide semiconductor (CMOS) cameras, each representing a Stokes component (0° and 90° for the horizontal channel, 45° and 135° for the tilted channel). The cameras are not used as imagers, instead the optical beams (+1 and −1 order) are projected onto the left and right side of each image, enabling a clear distinction between both diffracted orders. The optical elements are chosen in such a way that a maximum number of photons is bundled in as less pixels as possible, in order to increase the SNR.

For the instrument two, CS2100M-USB Quantalux 2.1 Megapixel Monochrome sCMOS cameras from Thorlabs are used.[15] These cameras

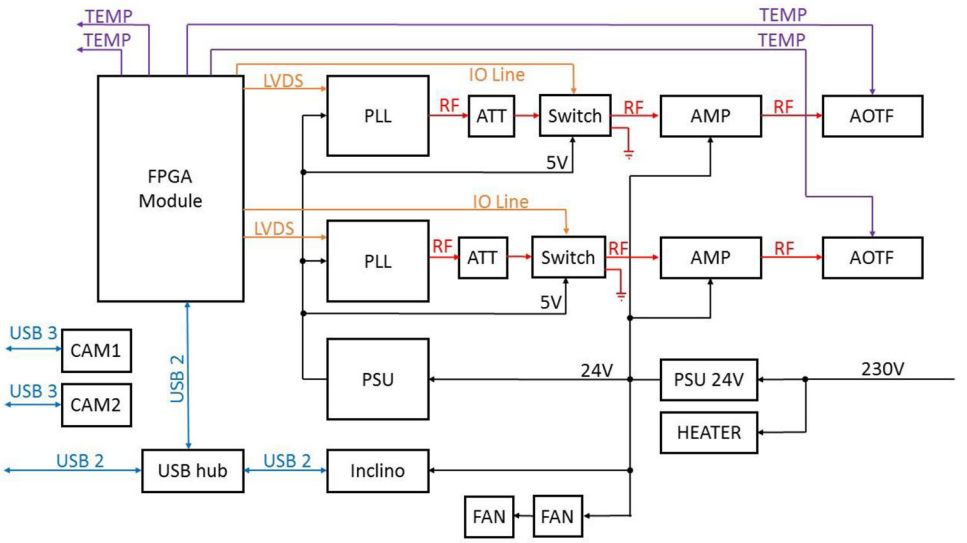

Figure 4. Block diagram of the ASPA-instrument.

are connected to an external laptop, using a USB 3.0-connection, enabling a separate readout of both channels (Figure 4).

Electronics

The instrument consists of different electrical elements. A block diagram is shown in Figure 4.

The RF generators need to be programed at the correct frequency. For this, a Spartan-6 field programmable gate array (FPGA) is used. This device drives the PLLs of both RF chains by using low-voltage differential signaling (LVDS). The FPGA is also responsible for the readout of the temperature probes. The inclinometer is used to determine the elevation of the instrument line of sight when pointing at auroras. The data is transferred using a USB connection.

Both AOTFs need a specific frequency and power level, hence, a double RF chain is designed (each driving an AOTF) containing an RF generator, an RF amplifier, and driving electronics. The RF generators are based on the PLL-principle, using an in-house designed frequency synthesizer – voltage controlled oscillator (VCO) combination to generate the appropriate frequencies for the two channels. Due to the fixed amplifier gain and the maximum allowable input signal, the RF generator output needs to be attenuated, before being applied to the RF amplifier (Figure 4) in order to achieve the desired output power levels. The initial generated output power of the RF chain lays much higher than the requested 60 mW (= +17.78 dBm) and 170 mW (= +22.30 dBm).

It is has been shown by Maák et al.[16] and Vanhamel et al.[17] that a portion of the applied RF energy is transformed into heat by the transducer of the AOTF. Hence, the RF chains not only need to compensate for the VSWR behavior, but also for the heat loss. Further, in each channel a switch is implemented, driven by the FPGA, using an input–output (IO)-line, to switch off the RF chain in order to make dark images of the observed scenery. This is necessary to remove any background noise in the final measurements. A power supply unit (PSU) is installed generating all applicable DC-voltage levels, using 230 V AC as input. This voltage is also directly used to power the heating system.

The laptop uses an in-house developed graphical user interface (GUI) to easily operate the instrument and to readout the inclinometer, using a USB connection (Figure 4). Several parameters can be adapted inside the GUI (e.g., frequency settings, integration time, and sweep boundaries) The software also assures that no RF is sent to the AOTFs at startup to avoid any damage to the transducers by connecting the RF to the ground using the switches.

Thermal balancing system

The instrument is designed to be used in the harsh environment of the polar regions. Temperatures can drop as low as 25 °C below zero. The used electronics are mostly commercial components, hence the environment in which they need to operate has to be above +5 °C. For this, a 90 W bi-metal feedback heater is installed inside a thermal box. This heater is self-regulated, using a bi-metal thermostat. Two small fans are set up inside the box in order to distribute the generated heat. The box itself is also isolated from the inside-out using isolation foam. Inside the metal enclosure, the temperature is monitored at four locations. Two probes are mounted onto the enclosure of the AOTFs to check for any increase in the temperature due to the heating of the transducers. This value is used in the calculations of the data to compensate for any frequency drift inside the AOTFs. The two remaining probes are fixed in the vicinity of the electronic boxes.

All optics and electronics are implemented inside a thermal box. For efficiently using the space inside the enclosure, both RF generators, the PSU and the FPGA module are stacked on top of each other.

Instrument test results

The performance of the instrument was tested beforehand, especially the output power level of the RF chains had to be characterized to assure a correct driving of the AOTFs. In addition, the temperature inside the

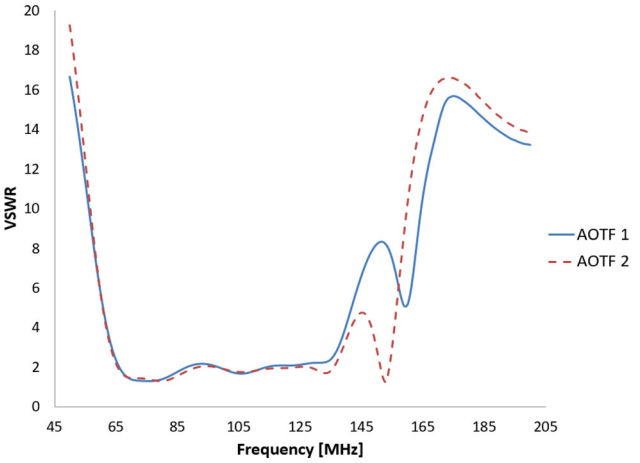

Figure 5. The voltage standing wave ratio (VSWR) properties of the two AOTFs under test.

thermal box has to be maintained at an acceptable level between +10 and +20 °C.

RF power output level and harmonic suppression

Both RF chains were subjected to power measurements. The desired output level must be 170 mW in the frequency domain from 80 to 105 MHz and 60 mW in the domain from 125 to 155 MHz. The VSWR values of both of the Gooch and Housego AOTFs were measured (Figure 5) using a vector-network analyzer. It is clear that both devices have a different VSWR behavior. Specifically in the upper-frequency region (140–160 MHz), the VSWR is relatively high (3:1 to 5:1). This region is used in the ASPA-instrument to measure the blue line (427.8 nm). Hence, the RF chains need to generate appropriate power levels to compensate for the power reflection. The higher power enables the conversion of an acceptable amount of energy at the transducer to have an effective optical efficiency level.

Due to the variable VSWR, the necessary RF chain output power level is dependent upon the frequency range. To compensate for this anomaly, together with the heating of the transducer,[16,17] different attenuator settings are used at the output of the RF generator enabling the RF amplifier to generate the different power levels, depending on the frequency domain (Figure 4). More specifically, to achieve the requested 60 mW (= +17.78 dBm) inside the crystal, the RF chain needs to generate an average of 174 mW (= +22.40 dBm) in the 80–105 MHz domain. In order to have 170 mW (= +22.30 dBm) inside the crystal, an average level of 871 mW (= +29.40 dBm) is necessary in the 125–155 MHz range.

The second and third harmonic level suppression for both AOTFs is measured in the two frequency ranges using a spectrum analyzer and is

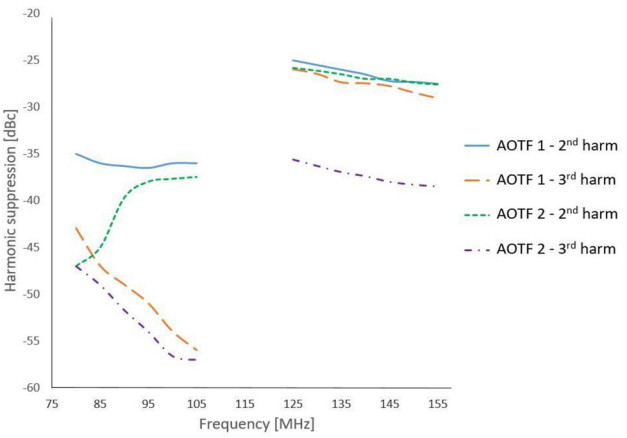

Figure 6. Second and third harmonics levels of the two RF chains in the applicable frequency regions.

shown in Figure 6. It is clear that the requirement of being below −25 dBc is reached for the second and third harmonics, and this in the complete frequency range.

Temperature measurements

During the assembly of the instrument, the feedback heating system was tested and performed well in a lab environment. Further testing at low temperatures was done during a field campaign. During these measurements, the temperature inside the metal enclosure was monitored at four different locations.

In Figure 7, the temperature variation as a function of time is shown for two probes mounted inside the instrument (probe #0 and probe #1). It is clear that, although the outside temperature was around −20 °C, the internal temperature was at a comfortable level (between +15 and +18.5 °C). The observed hysteresis is linked to the bi-metal thermostat of the heating system.

Conclusion and future work

The instrument was used in an international field test campaign in Skibotn, Norway, in February 2020, together with two other French teams. There it was placed on an observation deck, on top of the observatory of The Artic University of Norway (UIT). The mechanical box was mounted onto a solid tripod, able to withstand the wind gusts. During the campaign, the team was able to observe the auroral light several times. It is clear that the current setup must be seen as a proof of concept. Further adaptations are necessary in order to miniaturize the instrument to an acceptable level. The idea is to shrink the instrument toward a hand luggage sized box (55 × 40 × 20 cm, below 10 kg) in order to allow fluent and easy transportation by backpack, car, and airplane. In order to do this, the thermal box can be

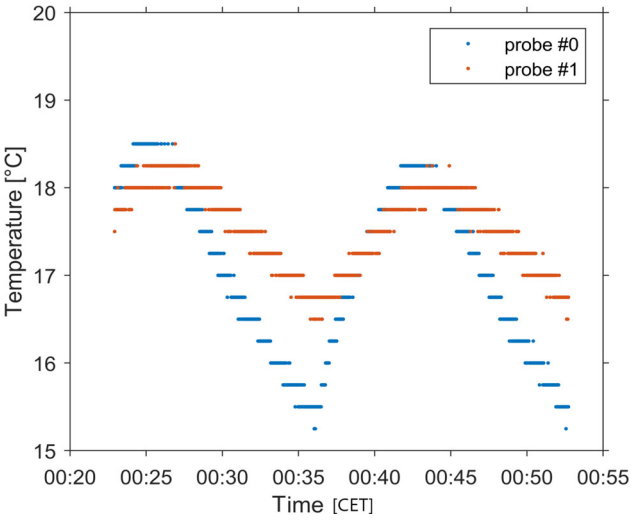

Figure 7. Temperature variations inside the thermal box of the ASPA-instrument measured in Central European Time (CET) [mm:ss] using two temperature probes (probe #0 and probe #1).

made smaller and lighter if the RF driving system and the driving electronics are adapted. This can be done for instance by using a digital RF driving system instead of the current PLL based setup. Integrating the capability to steer the RF power to the most optimal value (Figure 2) can lead to further optimization of the results. This is part of future work.

Acknowledgments

The authors would like to thank the engineering and solar radiation department for their performed work.

Disclosure statement

No potential conflict of interest was reported by the author(s).

Funding

This work was funded through the Prodex contract 4000110400.

ORCID

Jurgen Vanhamel http://orcid.org/0000-0002-0423-3309

References

[1] Dekemper, E.; Vanhamel, J.; Kastelik, J. C.; Pereira, N.; Bolsée, D.; Cessateur, G.; Lamy, H.; Fussen, D. New AOTF-Based Instrumental Concepts for Atmospheric Science. In *14th School on Acousto-Optics and Applications, Proceedings of SPIE 2019*, Torun, Poland, 24–27 June, 2019, 112100S-1–8. DOI: 10.1117/12.2540981.

[2] Lilensten, J.; Bommier, V.; Barthélemy, M.; Lamy, H.; Bernard, D.; Moen, J.; Johnsen, M. G.; Løvhaug, U. P.; Pitout, F. The Auroral Red Line Polarisation: Modelling and Measurements. *J. Space Weather Space Clim.* **2015**, *5*, A26–15. DOI: 10.1051/swsc/2015027.

[3] Lilensten, J.; Moen, J.; Barthélemy, M.; Thissen, R.; Simon, C.; Lorentzen, D. A.; Dutuit, O.; Amblard, P. O.; Sigernes, F. Polarization in Aurorae: A New Dimension for Space Environments Studies. *Geophys. Res. Lett.* **2008**, *35*, 1–5. DOI: 10.1029/2007GL033006.

[4] Barthelemy, M.; Lamy, H.; Vialatte, A.; Johnsen, M. G.; Cessateur, G.; Zaourar, N. Measurement of the Polarisation in the Auroral N_2^+ 427.8 nm Band. *J. Space Weather Space Clim.* **2019**, *9*, A26–8. DOI: 10.1051/swsc/2019024.

[5] Barthelemy, M.; Lystrup, M. B.; Menager, H.; Miller, S.; Lilensten, J. Is the Jovian Auroral H_3^+ Emission Polarised? *Astron. Astrophys.* **2011**, *530*, 1–12. DOI: 10.1051/0004-6361/201014314.

[6] Mortensen, A. N.; Dyer, S. A.; Hammaker, R. M.; Fateley, W. G. A Hadamard-Multiplexed Spectrometer Based on an Acousto-Optic Tunable Filter. *IEEE Trans. Instrum. Meas.* **1996**, *45*, 394–398. DOI: 10.1109/19.492754.

[7] Takahashi, H.; Masuda, C.; Gotoh, Y.; Koyama, J. Laser Diode Interferometer for Vibration and Sound Pressure Measurements. *IEEE Trans. Instrum. Meas.* **1989**, *38*, 584–587. DOI: 10.1109/19.192353.

[8] Dekemper, E.; Loodts, N.; Van Opstal, B.; Maes, J.; Vanhellemont, F.; Mateshvili, N.; Franssens, G.; Pieroux, D.; Bingen, C.; Robert, C.; et al. Tunable Acousto-Optic Spectral Imager for Atmospheric Composition Measurements in the Visible Spectral Domain. Appl. Opt. **2012**, *51*, 6259–6267. DOI: 10.1364/ao.51.006259.

[9] Montrone, L.; Aballea, L.; Bernaerts, D.; Navarro-Reyes, D.; Santandrea, S.; Saillen, N.; Sama, K.; Holbrouck, P.; Moelans, W.; Kendall, D.; et al. Technological Innovation for the ALTIUS Atmospheric Limb Sounding Mission. In *Sensors, Systems, and Next-Generation Satellites XXIII, Proceedings of SPIE 2019*, Strasbourg, France, Sep. 2019, 111510S-1–20. DOI: 10.1117/12.2533151.

[10] Yano, T.; Watanabe, A. Acoustooptic TeO(2) tunable filter using far-off-axis anisotropic Bragg diffraction. Appl. Opt. **1976**, *15*, 2250–2258. DOI: 10.1364/ao.15.002250.

[11] Jones, A. V. Auroral Spectroscopy. *Space Sci. Rev.* **1971**, *11*, 776–826. DOI: 10.1007/BF00216890.

[12] Sigernes, F.; Holmes, J. M.; Dyrland, M.; Lorentzen, D. A.; Svenøe, T.; Heia, K.; Aso, T.; Chernouss, S.; Deehr, C. S. Sensitivity Calibration of Digital Colour Cameras for Auroral Imaging. Opt. Express. **2008**, *16*, 15623–15632. DOI: 10.1364/OE.16.015623.

[13] Gupta, N.; Voloshinov, V. B. Development and Characterization of Two-Transducer Imaging Acousto-Optic Tunable Filters with Extended Tuning Range. Appl. Opt. **2007**, *46*, 1081–1088. DOI: 10.1364/AO.46.001081.

[14] Dekemper, E.; Vanhamel, J.; Van Opstal, B.; Fussen, D. The AOTF-Based NO_2 Camera. *Atmos. Meas. Tech.* **2016**, *9*, 6025–6034. DOI: 10.5194/amt-9-6025-2016.

[15] Thorlabs, CS2100M-USB Quantalux® 2.1 Megapixel Monochrome sCMOS Camera. https://www.thorlabs.com/thorproduct.cfm?partnumber=CS2100M-USB. (accessed June 10, 2020).

[16] Maák, P.; Takács, T.; Barócsi, A.; Kollár, E.; Richter, P. Thermal Behavior of Acousto-Optic Devices: Effects of Ultrasound Absorption and Transducer Losses. *Ultrasonics* **2011**, *51*, 441–451. DOI: 10.1016/j.ultras.2010.11.010.

[17] Vanhamel, J.; Dekemper, E.; Voloshinov, V. B.; Neefs, E.; Fussen, D. Electrical Bandwidth Testing of an AOTF Transducer as a Function of the Optical Diffraction Efficiency. *J. Opt. Soc. Am. A Opt. Image Sci. Vis.* **2019**, *36*, 1361–1366. DOI: 10.1364/JOSAA.36.001361.